8-1-2024

Expression of the αVβ3 Integrin Affects Prostate Cancer sEV Cargo and density and promotes sEV Pro-Tumorigenic Activity In Vivo Through a GPI-Anchored Receptor, NgR2

Cecilia Verrillo

Fabio Quaglia

Christopher Shields

Stephen Lin

Andrew Kossenkov

See next page for additional authors

Authors

Cecilia Verrillo, Fabio Quaglia, Christopher Shields, Stephen Lin, Andrew Kossenkov, Hsin-Yao Tang, David Speicher, Nicole Naranjo, Anna Testa, William Kelly, Qin Liu, Benjamin Leiby, Luca Musante, Khalid Sossey-Alaoui, Navneet Dogra, Tzu-Yi Chen, Dario Altieri, and Lucia Languino

Received: 3 July 2023 | Revised: 5 June 2024 | Accepted: 22 June 2024

DOI: 10.1002/jev2.12482

RESEARCH ARTICLE

Expression of the αVβ3 integrin affects prostate cancer sEV cargo and density and promotes sEV pro-tumorigenic activity in vivo through a GPI-anchored receptor, NgR2

Cecilia E. Verrillo[1,2] | **Fabio Quaglia**[1,2] | **Christopher D. Shields**[1,2] | **Stephen Lin**[1,2] | **Andrew V. Kossenkov**[3] | **Hsin-Yao Tang**[4] | **David Speicher**[4] | **Nicole M. Naranjo**[1,2] | **Anna Testa**[1,2] | **William K. Kelly**[5] | **Qin Liu**[6] | **Benjamin Leiby**[7] | **Luca Musante**[8] | **Khalid Sossey-Alaoui**[9] | **Navneet Dogra**[10] | **Tzu-Yi Chen**[10] | **Dario C. Altieri**[11] | **Lucia R. Languino**[1,2]

[1]Prostate Cancer Discovery and Development Program, Thomas Jefferson University, Philadelphia, Pennsylvania, USA

[2]Department of Pharmacology, Physiology, and Cancer Biology, Thomas Jefferson University, Philadelphia, Pennsylvania, USA

[3]Bioinformatics Shared Resource, Center for Systems and Computational Biology, The Wistar Institute, Philadelphia, Pennsylvania, USA

[4]Proteomics and Metabolomics Shared Resource, The Wistar Institute, Philadelphia, Pennsylvania, USA

[5]Department of Medical Oncology, Thomas Jefferson University, Philadelphia, Pennsylvania, USA

[6]Molecular and Cellular Oncogenesis Program, The Wistar Institute, Philadelphia, Pennsylvania, USA

[7]Division of Biostatistics, Department of Pharmacology, Physiology, and Cancer Biology, Sidney Kimmel Medical College, Thomas Jefferson University, Philadelphia, Pennsylvania, USA

[8]Extracellular Vesicle Core, PennVet, University of Pennsylvania, Philadelphia, Pennsylvania, USA

[9]Department of Medicine, Case Western Reserve University, School of Medicine MetroHealth Medical Center Rammelkamp Center for Research, Cleveland, Ohio, USA

[10]Department of Pathology and Cell Based Medicine, Icahn School of Medicine at Mount Sinai, New York, New York, USA

[11]Immunology, Microenvironment and Metastasis Program, The Wistar Institute, Philadelphia, Pennsylvania, USA

Correspondence
Lucia R. Languino, Bluemle Life Sciences Building 233 South 10th Street Suite 506, Philadelphia, PA 19107, USA. Email: lucia.languino@jefferson.edu

Funding information
Congressionally Directed Medical Research Programs, Grant/Award Number: DoD W81XWH2210826; Prostate Cancer Foundation, Grant/Award Number: Young Investigator Award; National Institutes of Health, Grant/Award Numbers: R01CA224769, R50CA211199, P30CA056036, R01CA217329, P20CA64076, P30CA010815, R01CA255792, R21AG078848, R50CA221838, R35CA220446; Thomas Jefferson University, Grant/Award Number: Philadelphia Prostate Cancer Biome Project

Abstract

It is known that small extracellular vesicles (sEVs) are released from cancer cells and contribute to cancer progression via crosstalk with recipient cells. We have previously reported that sEVs expressing the αVβ3 integrin, a protein upregulated in aggressive neuroendocrine prostate cancer (NEPrCa), contribute to neuroendocrine differentiation (NED) in recipient cells. Here, we examine the impact of αVβ3 expression on sEV protein content, density and function. sEVs used in this study were isolated by iodixanol density gradients and characterized by nanoparticle tracking analysis, immunoblotting and single vesicle analysis. Our proteomic profile of sEVs containing αVβ3 shows downregulation of typical effectors involved in apoptosis and necrosis and an upregulation of tumour cell survival factors compared to control sEVs. We also show that the expression of αVβ3 in sEVs causes a distinct reposition of EV markers (Alix, CD81, CD9) to a low-density sEV subpopulation. This low-density

Cecilia E. Verrillo and Fabio Quaglia contributed equally to this study.

reposition is independent of extracellular matrix (ECM) protein interactions with sEVs. This sEV subset contains αVβ3 and an αVβ3 downstream effector, NgR2, a novel marker for NEPrCa. We show that sEVs containing αVβ3 are loaded with higher amounts of NgR2 as compared to sEVs that do not express αVβ3. Mechanistically, we demonstrate that sEVs containing NgR2 do not affect the sEV marker profile, but when injected in vivo intratumorally, they promote tumour growth and induce NED. We show that sEVs expressing NgR2 increase the activation of focal adhesion kinase (FAK), a known promoter of cancer cell proliferation, in recipient cells. We also show that NgR2 mimics the effect of sEVs containing αVβ3 since it displays increased growth of NgR2 transfectants in vivo, as compared to control cells. Overall, our results describe the changes that occur in cargo, density and functions of cancer cell-derived sEVs containing the αVβ3 integrin and its effector, NgR2, without affecting the sEV tetraspanin profiles.

KEYWORDS
integrin, intratumoral injection of small extracellular vesicles, low-density small extracellular vesicles, neuroendocrine prostate cancer, NgR2, small extracellular vesicles

1 | INTRODUCTION

Extracellular vesicles (EVs) are delimited by a lipid bilayer and are heterogenous (Welsh et al., 2024). This paper focuses on small extracellular vesicles (sEVs), which are of endosomal or non-endosomal origin and are characterized by proteins such as CD9, CD81 and TSG101 (Mathieu et al., 2019). Most cell types, including cancer cells, release sEVs as a means of cell-cell communication (Peinado et al., 2017). The characteristics of sEVs differ depending on their density; low-density (LD) sEVs and high-density (HD) sEVs differentially express protein and DNA cargo (Kowal et al., 2016; Lázaro-Ibáñez et al., 2019) and have been shown to distinctly impact recipient cell gene expression (Willms et al., 2016).

sEVs have been studied in vitro for their ability to transfer proteins from tumour cells to recipient cells (Blavier et al., 2023; García-Silva et al., 2021; Singh et al., 2016). They are also being investigated as powerful biomarkers and possible therapeutic agents for prostate cancer (PrCa) (Krishn et al., 2019; Noren Hooten et al., 2020; Urabe et al., 2018; Urabe et al., 2024) which remains a predominant cause of cancer death among men in the United States (Siegel et al., 2024). A lethal form of PrCa is neuroendocrine prostate cancer (NEPrCa), which arises from treatment resistance or, in rare cases, de novo; patients diagnosed with NEPrCa are generally met with a poor prognosis and limited treatment options (Yamada & Beltran, 2021). NEPrCa has little to no androgen receptor and is associated with an increase in neuron-specific markers, including chromogranin A, Synaptophysin (SYP) and neuron-specific enolase (Beltran et al., 2011).

Integrins, receptors for the extracellular matrix (ECM), comprise two transmembrane subunits (α and β) (Quaglia et al., 2021). Integrins in sEVs have been identified as critical mediators of tumour growth (Lucotti et al., 2022) and organotropism (Hoshino et al., 2015). The αVβ3 integrin is known to be expressed in many aggressive cancers, to promote invasion and adhesion of cancer cells to ECM proteins, such as vitronectin and fibronectin (Desgrosellier & Cheresh, 2010; Zheng et al., 1999), and to protect disseminated tumour cells from chemotherapy (Carlson et al., 2019). Additionally, the αVβ3 integrin contributes to tumour cell survival in nutrient-deprived conditions (Nam et al., 2024). We have reported that the αVβ3 integrin is highly expressed in human and mouse NEPrCa but absent in prostate adenocarcinoma (ADPrCa) (Quaglia et al., 2021). In contrast, the αVβ6 integrin is present in ADPrCa (Lu et al., 2016) but negligible in NEPrCa (Quaglia et al., 2021). We have also reported that sEVs isolated from αVβ3 expressing PrCa cells induce neuroendocrine differentiation (NED) in recipient cells (Quaglia et al., 2020).

Our laboratory has recently reported that NgR2 (Nogo-66 receptor homolog 1), a member of the Nogo receptor family and a glycosylphosphatidylinositol (GPI)-anchored receptor, is upregulated by the αVβ3 integrin in a Kindlin-2 (K2)-dependent manner (Bledzka et al., 2016; Quaglia et al., 2022). We have also shown that NgR2 is upregulated in NEPrCa, promotes NED and cell motility and upregulates RhoA, a protein associated with aggressive phenotypes of PrCa (Quaglia et al., 2022; Schmidt et al., 2012). Previous studies have primarily investigated NgR2 as a neuronal protein (Barton et al., 2003) and as a receptor for two ligands: versican, a component of the ECM, and myelin-associated glycoprotein, a regulator of axonal growth (Bäumer et al., 2014; Venkatesh et al., 2005). We have shown that NgR2 is expressed in sEVs isolated from PrCa patient plasma (Testa et al., 2023), but the impact of NgR2-positive sEVs on recipient cancer cell differentiation has not been reported.

In this paper, we show that αVβ3 regulates NgR2 in sEVs and results in the formation of LD sEV subpopulations containing a unique cargo. We also show that intratumoral injection of αVβ3/NgR2+ sEVs induces tumour growth and NED in vivo. Overall,

our results describe the changes that occur in cargo, density and functions of cancer cell-derived sEVs containing the αVβ3 integrin and its effector, NgR2, without affecting the sEV tetraspanin profiles.

2 | MATERIALS AND METHODS

2.1 | Cell lines

PrCa cell lines (C4-2B, LNCaP, PC3, DU145) were cultured as previously described (Krishn et al., 2019, 2020). PC3 cells were transfected with sh*RTN4RL2* (SMARTvector, Dharmacon/Horizon, SO-2914049G, sequence: V3SVHS00_4716901 for sh*RTN4RL2*_1, V3SVHS00_7164907 for sh*RTN4RL2*_2 or V3SVHS00_8801245 for sh*RTN4RL2*_3) or shSCRAMBLE (SMARTvector, Dharmacon/Horizon, VSC11707) and were selected using 2 μg/mL puromycin, as previously described (Quaglia et al., 2022). DU145 cells were transfected with a pCMV6-Entry vector carrying *RTN4RL2* (Origene, SC310413) or an empty vector (Origene, PS100001), designated as NgR2-DU145 or Mock-DU145 cells, as previously described (Quaglia et al., 2022). Briefly, cells were plated at 5×10^5 cells/well in serum-free DMEM media and incubated with 4 μg of vector DNA and 12 μL of Lipofectamine™ 2000 (Invitrogen, 11668-019). Successfully transfected cells were selected using 0.5 mg/mL G418. C4-2B and LNCaP PrCa cells were transfected for αVβ3 expression (αVβ3-C4-2B and αVβ3-LNCaP) or Mock control (Mock-C4-2B and Mock-LNCaP), as previously described (Quaglia et al., 2020). Kindlin-2 (K2) knock-out (KO) cells were generated using a single-guided RNA, as previously described (Quaglia et al., 2022). Homozygous CRISPR-Cas9 KO clones for NgR2 (PC3 NgR2 KO) and PC3 Control cells were purchased from Synthego (Synthego Corporation, Menlo Park, California). Guide RNA sequence 5′-AUCGAGACAAGAUGCUGCCC-3′ was used to generate PC3 NgR2 KO cells; PC3 control cells were mock-electroporated with Cas9 only.

2.2 | Antibodies

The following antibodies (Abs) were used for immunoblotting (IB) analysis: goat polyclonal Ab against NgR2 (AF2776, R&D Systems), mouse monoclonal Abs against Kindlin-2 (MAB2617, Sigma), CD9 (sc-13118, Santa Cruz), CD81 (ab23505, Abcam), CD63 (ab193349, Abcam) and Alix (ab117600, Abcam), rabbit monoclonal Abs against β3 (13166S, Cell Signaling) and Syntenin (ab133267, Abcam), rabbit polyclonal Abs against Actin (a2066, Sigma), Calnexin (2433S, Cell Signaling), Fibronectin (sc-9068, Santa Cruz), FAK (sc-558, Santa Cruz), FAK^{pY397} (44-624G, Invitrogen), RhoA (sc-179, Santa Cruz), TSG101 (ab30871, Abcam) and αV [rabbit serum, (Trerotola et al., 2013)]. The following Ab was used for ExoView analysis: Alexa-555 mouse monoclonal Ab against αVβ3 (LM609, MAB1976-AF555, Sigma). The following Abs were used for immunohistochemical analysis: rabbit polyclonal Abs against NgR2 (PA5-98577, Invitrogen), Synaptophysin (PA1-1043, Invitrogen) and non-immune rabbit IgG (I5006, Sigma).

2.3 | Immunoblotting analysis

IB analysis was performed as previously described (Krishn et al., 2020).

2.4 | sEV isolation by differential ultracentrifugation and iodixanol density gradient separation

Cells were plated in 20–30 150 mm plates (1×10^7 cells/plate) and cultured in serum-free medium (15 mL/plate) for 48 h. The culture supernatant was collected, and EVs were isolated by differential ultracentrifugation three consecutive times. Differential ultracentrifugation and iodixanol density gradient (IDG) separation were performed as previously described (Quaglia et al., 2020). Briefly, the collected cell supernatant was spun for 20 min at 2000 × *g* (4°C). The spun supernatant was transferred to ultracentrifuge tubes (Beckman Coulter) and centrifuged using a Type 45 Ti rotor (Beckman Coulter) for 35 min at 10,000 × *g* (4°C). The pellet was discarded, and the supernatant was spun for 70 min at 100,000 × *g* (4°C); the resulting EV pellet was collected by resuspending in PBS. This process was repeated thrice; the collected EV samples were pooled and spun for 70 min at 100,000 × *g* (4°C), and the resulting pellet was resuspended in iodixanol buffer (0.25 M sucrose, 10 mM Tris, 1 mM EDTA, pH 7.4). For IDG separation, a discontinuous gradient was formed by diluting 30%, 20% and 10% iodixanol solutions (wt/vol) from a 60% wt/vol iodixanol stock solution (OptiPrep™, Sigma) with iodixanol buffer. EVs, collected by differential ultracentrifugation, were included in the 30% wt/vol solution and loaded to the bottom of an 11 × 60 mm centrifuge tube (Seton), followed by 20% wt/vol and 10% wt/vol solutions. The discontinuous gradient was then centrifuged for 70 min at 350,000 × *g*

(4°C). Ten fractions were collected, washed with 1 mL PBS and centrifuged for 70 min at 100,000 × *g* (4°C). The subsequent pellets were resuspended in PBS and analysed.

2.5 | Trypsinization of sEVs

Pooled EV samples collected by differential ultracentrifugation were spun at 100,000 × *g* for 70 min (4°C). Sample supernatants were removed, and EV pellets were resuspended in trypsin (0.05% trypsin, 0.53 mM EDTA, Fisher) and incubated at RT for 90 s. Neutralization of the reaction was performed using 1 mg/mL soybean trypsin inhibitor (Gibco). The neutralized EV samples were immediately resuspended in iodixanol buffer and IDG separation was performed as described in Section 2.4.

2.6 | Nanoparticle tracking analysis

Nanoparticle tracking analysis (NTA) was performed as previously described (Quaglia et al., 2020). Briefly, pooled iodixanol fractions (~100 μL sample) were diluted 1:200 in PBS and analysed using NanoSight NS300. Samples were captured in three 30-s videos. Data were collected at 25°C, detection threshold 5 and a camera level ranging from 11 to 13. Samples were run using a syringe pump to ensure consistent motion. Data analysis was performed using NTA software version 3.1 (build 3.1.54).

2.7 | Proteomic analysis—Liquid chromatography–tandem mass spectrometry (LC–MS/MS) analyses and data processing

Replicates of $\alpha V\beta 3$-C4-2B or Mock-C4-2B sEV samples (11 μg each) were run into a NuPAGE 10% Bis-Tris gel (Thermo Scientific) and fractionated into 3 gel slices for trypsin digestion followed by liquid chromatography–tandem mass spectrometry (LC–MS/MS) analysis, as previously described (Hao et al., 2024). Proteins and peptides were identified using MaxQuant 1.6.3.3 (Cox & Mann, 2008) by searching the MS/MS spectra against the UniProt human protein database. Missing values were replaced with a small value, and fold change was calculated from the Log2 values. Protein and peptide identifications were generated with false discovery rates set at 1%.

The dataset for NEPrCa and CRPrCa (Beltran et al., 2016) was downloaded from cBioPortal [dataset: *Neuroendocrine Prostate Cancer (Multi-Institute, Nat Med 2016)*] and analysed as follows: FPKM values were log2 transformed and limma package (Ritchie et al., 2015) was used to estimate significance of differential expression between the two groups. The analysis identified 982 differentially expressed genes (FDR < 10%). Ingenuity Pathway Analysis [IPA (Cox & Mann, 2008)] was used to find known targets of proteins identified from proteomics analysis and the resulting gene set was analysed for pathway enrichment. Select pathways that had predicted activation *Z* score of at least 2 were reported.

2.8 | Single vesicle analysis via ExoView R100

sEVs were analysed using ExoView R100 (Unchained Labs, Inc.) according to the manufacturer's protocol. sEVs were diluted 1:5000–1:10,000 using ExoView incubation buffer and incubated on chips from ExoView human tetraspanin kits (215-1000, Unchained Labs) overnight. Chips, seeded with capture Abs to CD63, CD81, CD9 and mIgG in triplicate, were pre-scanned prior to sEV incubation. After sEV incubation, chips were washed three times with ExoView solution A and incubated for 1 h with fluorescently labelled Abs: Alexa 647-Ab to CD63, Alexa 555-Ab to CD81 and Alexa 488-Ab to CD9 or Alexa 555-609-Ab to $\alpha V\beta 3$ in ExoView blocking buffer. Chips were washed once in ExoView solution A, three times in ExoView solution B, and one time with DI water. Chips were dried and read using ExoView R100 reader and analysed using ExoView software suite (v3.2.1). The captured spots were manually examined during the quality control steps, and outliers were removed. The cut-off was established on the mIgG isotype controls and maintained across experiments (Deng et al., 2022). Particle count was normalized by restricting the analysis to an area of a 150 μm circle.

2.9 | Animal care

SCID CB-17 mice (Charles River) were cared for and monitored according to Office of Laboratory Animal Welfare, NIH, and Department of Health and Human Services standards. Institutional Animal Care and Use Committee recommendations were followed, and all protocols were approved by the Institutional Animal Care and Use Committee at Thomas Jefferson University.

2.10 | Intratumoral sEV injection

SCID CB-17 mice were subcutaneously injected with 2×10^6 DU145 cells, and tumour volume was measured twice a week using a calliper. sEVs were injected intratumorally once tumour volume reached 100 mm^3. sEVs resuspended in PBS from NgR2-DU145 cells, Mock-DU145 cells or PBS as control were injected intratumorally two consecutive times (10 μg/injection) three times a week. Mice were euthanized 14 days following the initial sEV injection; tumour weight was measured after sacrifice.

2.11 | sEV transfer to PrCa cells

sEVs were isolated from PC3 sh*RTN4RL2*, PC3 shScramble, PC3 NgR2 KO or PC3 Control cells as described in section 2.4. For sEV transfer, LNCaP or DU145 PrCa cells were plated 3×10^5 cells/well in 6-well plates and incubated (37°C, 5% CO_2) in DMEM for 24 h. After 24 h, LNCaP cells were washed with PBS and incubated with 10 μg/mL PC3 sh*RTN4RL2* or PC3 shScramble sEVs resuspended in media depleted of fetal bovine serum (FBS); DU145 cells were washed with PBS and incubated with PC3 NgR2 KO or PC3 Control sEVs (1×10^9 sEVs/mL) resuspended in media depleted of FBS. Incubation with PBS resuspended in media depleted of FBS was used as a negative control. After a 24-h incubation, cells were washed three times with PBS, harvested via scraping and analysed by IB.

2.12 | Effects of NgR2 expression on tumour growth

SCID CB-17 mice were subcutaneously injected with 2×10^6 NgR2-DU145, Mock-DU145, PC3 sh*RTN4RL2*_3, PC3 sh*RTN4RL2*_2, PC3 sh*RTN4RL2*_1 or PC3 shScramble transfectants. Mice were monitored twice a week, and tumour volume was measured using a calliper. All mice were sacrificed once a tumour volume of 2×10^3 mm^3 was reached. Tumour weight was measured after sacrifice.

2.13 | Immunohistochemical analysis

Tumour xenografts [DU145 tumours injected with sEVs (NgR2-DU145 sEVs, Mock-DU145 sEVs) or tumours from PC3 sh*RTN4RL2*_3, or PC3 shScramble cells] were analysed using immunohistochemical (IHC) analysis, as previously described (Quaglia et al., 2022).

2.14 | *RTN4RL2* expression in PrCa patient cohort

Gene expression data from Chen et al. (2022) of isolated EVs (serum EVs $n = 24$, urine EVs $n = 7$) from PrCa patients were analysed. Tumour tissue ($n = 5$) and normal tissue ($n = 5$) gene expression data from Chen et al. (2022) were also analysed. For quantification of gene expression, raw RNA reads were aligned using the ExceRpt pipeline for small RNAs, including the filtering and automatic adaptor removal steps. Briefly, ExceRpt uses STAR aligner versions 2.4 and above to align the reads to multiple references to identify contaminants and applies a moderate filter, removing low-quality and multimapping reads. The final product ExceRpt was a count matrix displaying each sample in columns and genes in rows. After mapping we used edgeR and limma packages for differential expression analysis. We considered a threshold of at least ten counts across all samples as a filter with an upperQuantile normalization (normalized transcripts per million values for each gene). Normalized mRNA expression of the *RTN4RL2* gene across all samples is plotted, and the p value is determined via paired Wilcoxon test.

2.15 | Statistical analysis

Tumour weights and changes from baseline in tumour volume at the end of each experiment were examined to determine the treatment effect. For two group comparisons, t-test or Mann–Whitney test was used. For experiments with three groups, Kruskal–Wallis test or ANOVA with post-hoc Tukey's multiple comparisons test was used. Longitudinal tumour measurements were log-transformed and modelled using mixed effects linear regression to compare tumour growth rates. Data were analysed using SAS 9.4 or GraphPad Prism 9.

3 | RESULTS

3.1 | NgR2 expression in sEVs secreted from αVβ3-positive prostate cancer cells—proteomic analysis of sEVs

We have shown that sEVs released by prostate cancer (PrCa) cells contain the αVβ3 integrin and promote a neuroendocrine (NE) phenotype in recipient PrCa cells both in vitro and in vivo (Quaglia et al., 2020). We have also previously shown that the αVβ3 integrin increases the levels of NgR2, which is a receptor upregulated in NEPrCa that promotes neuroendocrine differentiation (NED) (Quaglia et al., 2022). To investigate whether NgR2 levels are increased in αVβ3-positive sEVs, we isolated sEVs using iodixanol density gradients (IDGs) from the serum-free culture media of two PrCa cells, C4-2B and LNCaP, exogenously expressing the αVβ3 integrin (αVβ3-C4-2B and αVβ3-LNCaP, respectively) and compared them to their respective Mock transfectants (Mock-C4-2B and Mock-LNCaP) (Figure 1a–c). Nanoparticle tracking analysis (NTA) provides evidence that the average sEV size falls below 200 nm in cell transfectants from both cell types (Figure 1a). Additionally, immunoblotting (IB) analysis of αVβ3-C4-2B, Mock-C4-2B, αVβ3-LNCaP and Mock-LNCaP sEVs shows the expression of sEV markers (Alix, TSG101 and CD9). All sEVs analysed do not express calnexin (CANX), a marker of the endoplasmic reticulum (ER). Overall, we conclude that the increased levels of NgR2 in αVβ3-positive sEVs reflect the pattern of expression observed in αVβ3-positive cells [Figure 1b and c; (Quaglia et al., 2022)].

To analyse the impact of αVβ3 on sEV cargo, we performed proteomic analysis of sEVs released by αVβ3-C4-2B cells and compared them to Mock-C4-2B sEVs. We identified 33 proteins upregulated at least 5-fold in αVβ3-C4-2B sEVs versus Mock-C4-2B sEVs (Figure 1d). As expected, the αVβ3 integrin was confirmed to be upregulated in αVβ3-C4-2B sEVs. The β3 subunit (encoded by the *ITGB3* gene) was upregulated at least 5-fold; the αV subunit (encoded by the *ITGAV* gene) was also significantly upregulated 2.6-fold in αVβ3-C4-2B sEVs when compared to Mock-C4-2B sEVs ($p = 0.033$, not depicted). Among these 33 upregulated proteins, the cell surface receptor NgR2 (encoded by the *RTN4RL2* gene) was verified as a downstream effector of the αVβ3 integrin. Gene expression analysis of NEPrCa versus castrate-resistant prostate cancer (CRPrCa) reported in Beltran et al. (2016) identifies 982 genes differentially expressed in a significant manner (FDR < 10%) in CRPrCa versus NEPrCa; of these, we identified 181 known targets of at least one of the 33 proteins upregulated in sEVs expressing the αVβ3 integrin, with 21 of those related to cell proliferation (Figure 1e). Moreover, Ingenuity Pathway Analysis [IPA (Krämer et al., 2014)] of the 181 genes shows inhibition of apoptosis and necrosis, and activation of neuronal cell functions, cancer survival, G1 phase and stem cell differentiation (Figure 1f).

3.2 | Aberrant cargo and density of sEVs released from αVβ3-positive prostate cancer cells

Our analysis of sEVs isolated via IDG (Figure 2a) shows that expression of αVβ3 in C4-2B cells causes all sEV markers to be enriched in a low-density (LD) subpopulation. The red boxes indicate the LD fractions of αVβ3-C4-2B (left panel) and Mock-C4-2B (right panel) sEVs; the black dotted boxes indicate the fractions that show enrichment of sEV markers Alix, CD81 and CD9 in αVβ3-C4-2B and Mock-C4-2B sEVs. As indicated by the change in position of the dotted boxes, sEV markers are specifically enriched in a LD subpopulation in αVβ3-C4-2B sEVs (Figure 2a, S1a–c). In addition to the enrichment of NgR2, αVβ3-C4-2B sEVs are also enriched in RhoA, a protein associated with aggressive phenotypes of PrCa (Schmidt et al., 2012). Both αVβ3-C4-2B and Mock-C4-2B sEVs also express the tetraspanin CD63; furthermore, αVβ3-C4-2B sEVs show αV expression (not shown). These results indicate that the αVβ3 integrin co-fractionates with NgR2 in sEVs, suggesting that the interaction between these two proteins, previously shown in cells (Quaglia et al., 2022), remains stable in sEVs.

In parallel, the interaction of the αVβ3 integrin with the ECM protein fibronectin (FN) was analysed as a potential component of the enrichment of LD sEVs isolated from αVβ3-C4-2B cells. αVβ3-C4-2B cells, Mock-C4-2B cells, their respective sEVs and FN were analysed by IB with Abs against FN, β3, CD9 and CANX (Figure 2b). Additionally, αVβ3-C4-2B and Mock-C4-2B sEVs were trypsinized to cleave FN from the surface of sEVs and subsequently separated by IDG. Both αVβ3-C4-2B cells and their respective sEVs show FN enrichment when compared to Mock-C4-2B. In contrast, FN is absent in trypsinized αVβ3-C4-2B and Mock-C4-2B sEVs. Moreover, IB analysis of the individual IDG fractions of trypsinized αVβ3-C4-2B sEVs shows that the sEVs remain enriched in a LD subpopulation (Figure 2c, respective densities shown in Figure 2d).

The αVβ3 co-activator Kindlin-2 (K2) is also detectable at higher levels in the sEVs isolated from αVβ3-C4-2B as compared to Mock-C4-2B sEVs (Figure 2a). We have previously shown that αVβ3 expression does not affect K2 levels in cells (Quaglia et al., 2022), but here we show that αVβ3 contributes to the enrichment of K2 in sEVs. In parallel, we tested if the downregulation of K2 affects αVβ3 levels in sEVs. As previously reported (Quaglia et al., 2022), PC3 cells were incubated with a single-guided RNA against K2 (sgK2) or the control counterpart (sgControl). sgControl or sgK2 lysates and a pool of the first five fractions of their derived sEVs, isolated by IDG (Figure 2e), were analysed by IB with Abs to β3, K2, CD9, CD81 and CANX. The results show that the downregulation of K2 does not affect αVβ3 levels in sEVs. We also show, through single vesicle analysis, that the incubation

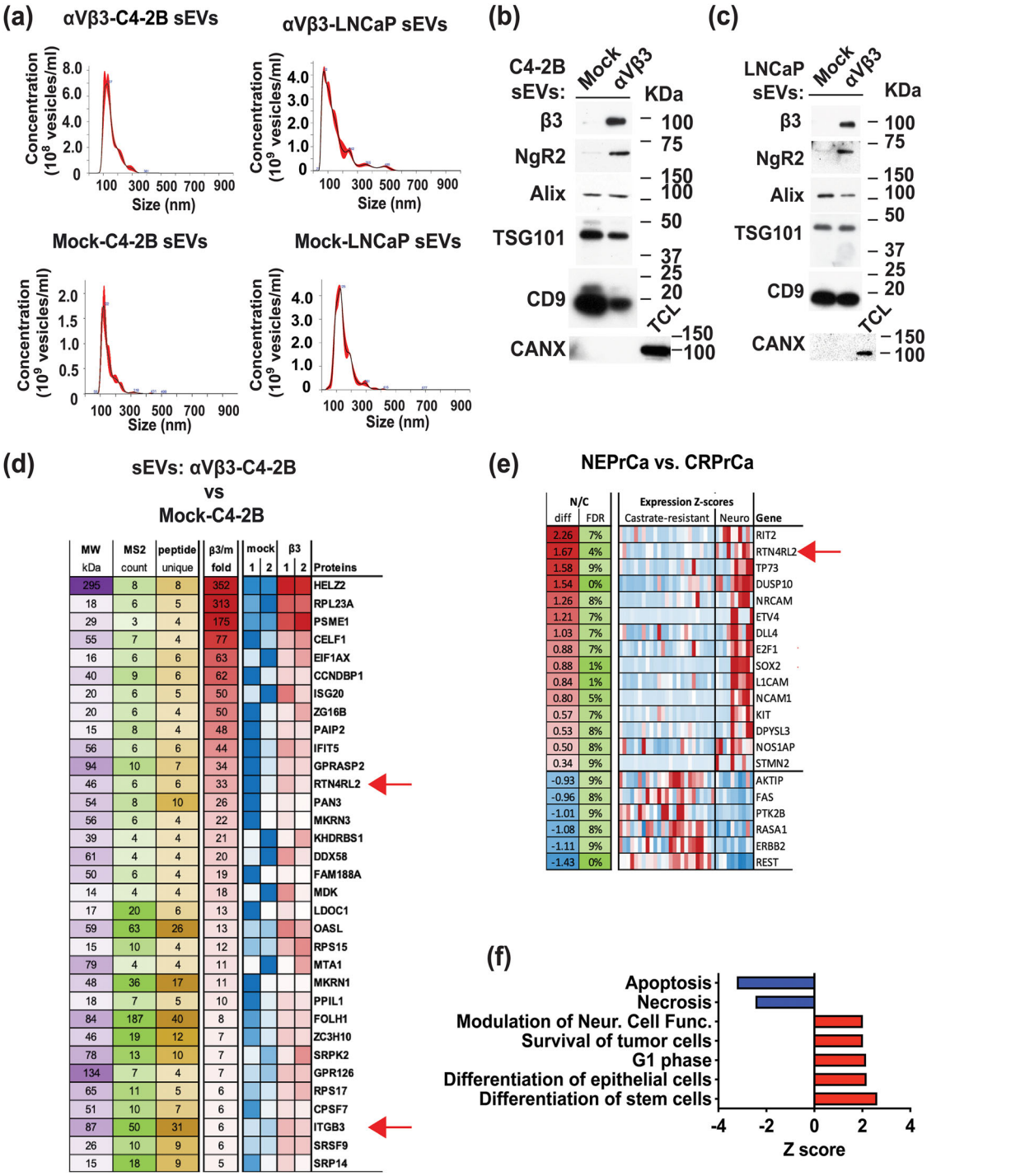

FIGURE 1 Proteomic analysis of αVβ3-C4-2B sEVs and Mock-C4-2B sEVs. (a) Nanoparticle tracking analysis (NTA) of sEVs isolated via iodixanol density gradient (IDG) from prostate cancer (PrCa) cells exogenously expressing αVβ3 (αVβ3-C4-2B or αVβ3-LNCaP) or a negative control vector (Mock-C4-2B or Mock-LNCaP); αVβ3-C4-2B sEVs (top left panel), Mock-C4-2B sEVs (bottom left panel), αVβ3-LNCaP sEVs (top right panel) and Mock-LNCaP sEVs (bottom right panel) are shown, $n = 2$ biological replicates for each condition. (b-c) sEVs isolated from αVβ3 and Mock transfectants were analysed by immunoblotting (IB). Expression of β3, NgR2, Alix, TSG101, CD9 and Calnexin (CANX) was analysed. Total cell lysate (TCL) was used as a positive control for CANX. (b) IB results of Mock-C4-2B and αVβ3-C4-2B sEVs. (c) IB results of Mock-LNCaP and αVβ3-LNCaP sEVs. (d) Expression heatmap of 33 high-confidence proteins identified as upregulated at least 5-fold in αVβ3-C4-2B versus Mock-C4-2B sEVs. (e) Expression heatmap of genes related to cell proliferation that are significantly upregulated in neuroendocrine (NE) versus castrate-resistant (CR) PrCa (top section) or downregulated in NE versus CR PrCa (bottom section). (f) Activation *Z* scores for functions enriched among genes significantly affected in NEPrCa that are known targets of proteins upregulated in αVβ3-C4-2B versus Mock-C4-2B sEVs, characterized by ingenuity pathway analysis.

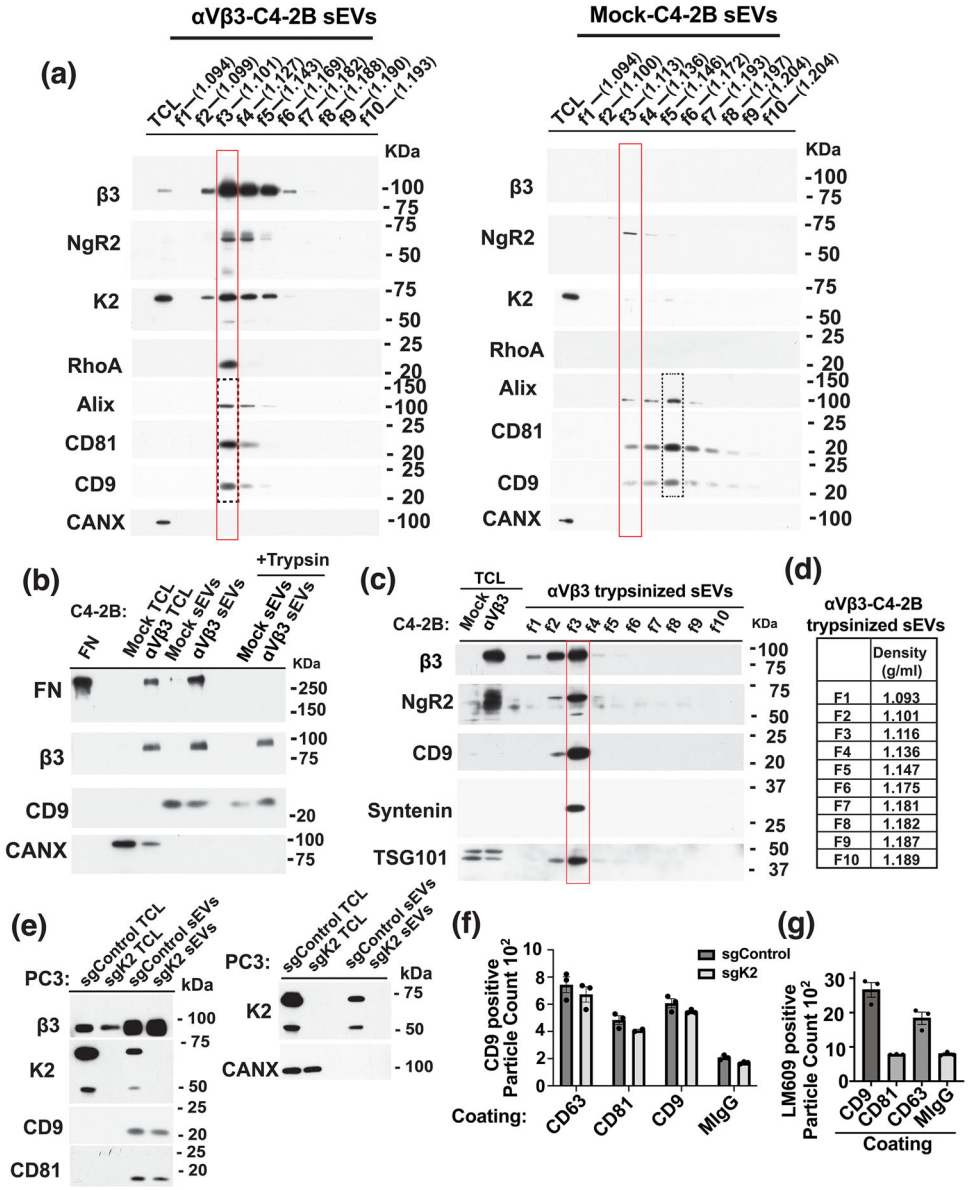

FIGURE 2 Expression of αVβ3 shifts sEV markers to a lower density sEV subpopulation. (a) sEVs were isolated from the supernatant of αVβ3-C4-2B (left panel) and Mock-C4-2B (right panel) PrCa cell transfectants via IDG separation. Fractions 1–10 were analysed through IB; each fraction is labeled with its respective density (g/mL). sEVs and TCL were characterized for expression of β3, NgR2, Kindlin-2 (K2), RhoA, Alix, CD81, CD9 and CANX. Red boxes indicate the low-density (LD) fractions of αVβ3-C4-2B (left panel) and Mock-C4-2B (right panel) sEVs; the black dotted boxes indicate the fractions that show enrichment of sEV markers Alix, CD81 and CD9 in αVβ3-C4-2B and Mock-C4-2B sEVs. (b) IB analysis of trypsinized and non-trypsinized sEVs isolated from Mock-C4-2B and αVβ3-C4-2B cells. Fibronectin (FN), Mock-C4-2B TCL and αVβ3-C4-2B TCL were also analysed for expression of FN, β3, CD9 and CANX. (c) Trypsinized αVβ3-C4-2B sEVs isolated by IDG, lysates from Mock-C4-2B and αVβ3-C4-2B cells were also analysed by IB for expression of β3, NgR2, CD9, Syntenin and TSG101. (d) Densities (g/mL) of IDG fractions 1–10 of trypsinized αVβ3-C4-2B sEVs are shown. (e) sEVs were isolated from sgK2 and sgControl PC3 cells by IDG separation into ten fractions; sEV fractions 1–5 were pooled for analysis. sgControl or sgK2 TCLs and sEVs were analysed by IB using Abs to β3, K2, CD9, CD81 (left panel) and CANX (right panel). (f) ExoView analysis of sEVs isolated from PC3 sgK2 or PC3 sgControl cells. sEVs were captured on chips coated in triplicate with Abs against CD63, CD81, CD9 and MIgG and analysed for CD9, detected using Alexa 488-Ab against CD9. (g) ExoView analysis of sEVs isolated from PC3 cells. sEVs were captured on chips coated in triplicate with Abs against CD63, CD81, CD9 and MIgG. Normalized particle count of αVβ3-positive sEVs, detected using Alexa 555-Ab LM609 against αVβ3 is shown. Particle counts were normalized as described in Materials and Methods Section 2.8.

of sgK2 does not impact sEV tetraspanin profiles (CD63, CD81 and CD9) when compared to sgControl (Figure 2f). In addition, we show through ExoView analysis of PC3 sEVs, that αVβ3 is expressed on the surface of sEVs (Figure 2g) and is recognized by LM609, an inhibitory Ab to a unique αVβ3 epitope. This Ab is bound most abundantly to sEVs captured by the CD9 and CD63 Abs, and less by sEVs bound to the CD81 capture spot. Overall, these data show that αVβ3 expression causes aberrant cargo loading and density of sEVs secreted from PrCa cells without affecting the sEV tetraspanin profiles.

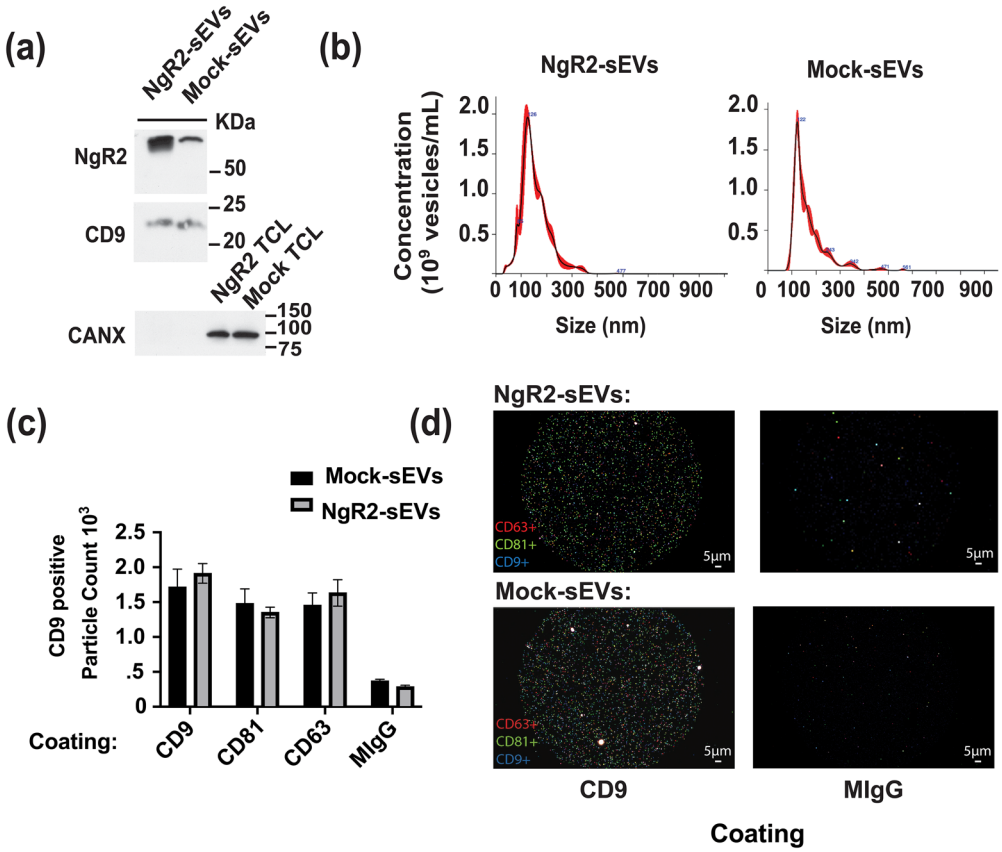

FIGURE 3 Characterization of sEVs isolated from NgR2-DU145 PrCa cells. (a) IB of sEVs isolated from NgR2-DU145 and Mock-DU145 transfectants via IDG; fractions 2–5 were pooled, lysed and analysed using Abs to NgR2, CD9 and CANX. NgR2-DU145 sEVs (NgR2-sEVs) were compared to control Mock-DU145 sEVs (Mock-sEVs); NgR2-DU145 and Mock-DU145 TCLs were used as a positive control for CANX. (b) NTA of NgR2-sEVs and Mock-sEVs ($n = 2$ biological replicates for each condition). (c,d) Single vesicle characterization of NgR2-sEVs and Mock-sEVs by ExoView. (c) Comparison of normalized number of particles positive for CD9 of NgR2-sEVs and Mock-sEVs, detected using Alexa 488-Ab against CD9 using capture Abs to CD9, CD81, CD63 and MIgG ($n = 3$). Particle counts were normalized as described in the Materials and Methods Section 2.8. (d) Representative images of NgR2-sEVs and Mock-sEVs captured on CD9 Ab or MIgG coated chips. Binding of sEVs to mAbs against CD63 (Alexa 647-Ab; red), CD81 (Alexa 555-Ab; green) and CD9 (Alexa 488-Ab; blue) was analysed. White = CD63 (Alexa 647-Ab; red), CD81 (Alexa 555-Ab; green) and CD9 (Alexa 488-Ab; blue); cyan = CD81 (Alexa 555-Ab; green) and CD9 (Alexa 488-Ab; blue); yellow = CD63 (Alexa 647-Ab; red), CD81 (Alexa 555-Ab; green); purple = CD63 (Alexa 647-Ab; red) and CD9 (Alexa 488-Ab; blue). The bar in each image represents 5 μm.

3.3 | Transfer of NgR2-positive sEVs to recipient cells increases tumour growth

We investigated whether the transfer of sEVs that contain NgR2 to recipient cells increases tumour growth. For this purpose, we isolated sEVs via IDG from DU145 cells exogenously expressing NgR2 (NgR2-sEVs) and compared them to control Mock-DU145 sEVs (Mock-sEVs). NgR2-sEVs as well as Mock-sEVs were analysed by IB for NgR2, CD9 and CANX expression (Figure 3a); the results show that the levels of CD9 are comparable (Figure 3a), and NTA shows that the average size of both sEV types is = to or < 200 nm (Figure 3b). Similarly, single vesicle characterization (Figure 3c) shows that NgR2-sEVs and Mock-sEVs express comparable levels of CD9 and bind equally well to CD9, CD81 and CD63 Abs. Images of both sEVs captured on the CD9-Ab coated chip also show similar expression of tetraspanins CD63, CD81 and CD9 (Figure 3d).

To visualize the transfer of NgR2 to recipient cells in vitro, LNCaP cells, selected for their low levels of NgR2 expression, were incubated with sEVs isolated from PC3 cells transfected with shRNA against NgR2 (shRTN4RL2) or scramble shRNA, characterized previously (Quaglia et al., 2022; Testa et al., 2023). Cells were incubated with sEVs for 24 h, lysed, and analysed by IB for Abs against NgR2, RhoA and CANX (Figure 4a). The recipient cell expression of NgR2 increases upon incubation of NgR2-positive (shScramble) sEVs when compared to sh*RTN4RL2* sEVs. This result indicates that NgR2 is transferred from NgR2-positive sEVs to recipient cells. Additionally, NgR2-positive sEVs increase recipient cell expression of RhoA.

To analyse the effects of NgR2-positive sEVs on tumour growth in vivo, NgR2-sEVs and Mock-sEVs were intratumorally injected into DU145 tumours grown in SCID mice to a tumour size of 100 mm^3 (n = 9/group). PBS was used as a negative control (n = 11). Tumour volume was measured every 3 days, for 14 days after the initial injection of sEVs, and final tumour weight was measured at the time of sacrifice. The result shows that NgR2-sEVs significantly increase ($p < 0.0001$) tumour volume

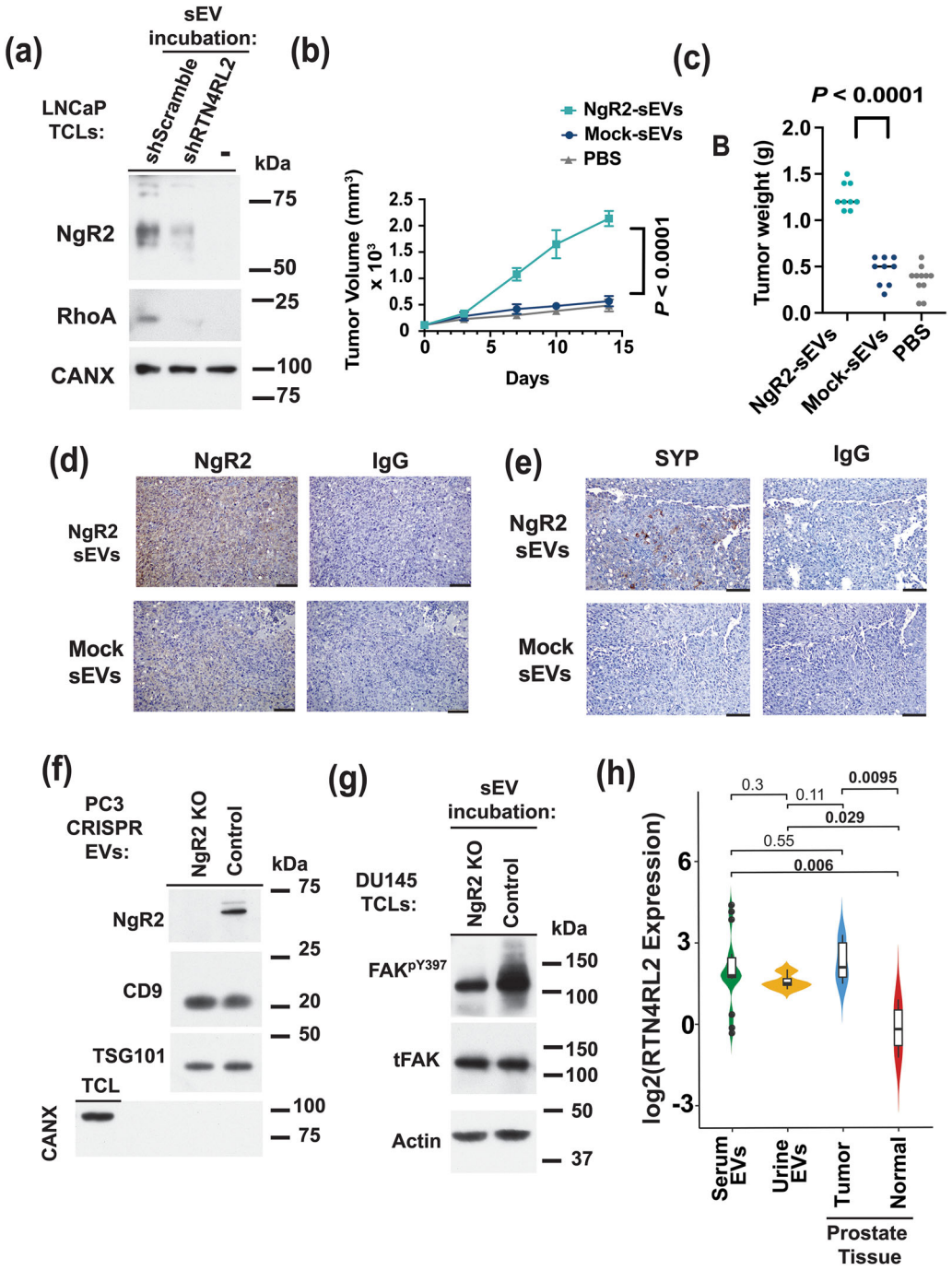

FIGURE 4 Transfer of NgR2+ sEVs to recipient cells increases tumour growth and Synaptophysin expression. (a) IB analysis of LNCaP TCLs collected 24 h after sEV incubation. Samples were incubated with PBS (−) or incubated with 10 μg/mL PC3 shScramble or PC3 sh*RTN4RL2* sEVs. Samples were analysed for expression of NgR2, RhoA and CANX. (b) DU145 cells (2×10^6) were subcutaneously injected in SCID mice and grown to a tumour size of 100mm^3. Once grown, intratumoral injection with NgR2-sEVs ($n = 9$), Mock-sEVs ($n = 9$) or PBS ($n = 11$) as a negative control, was performed. Tumour volume was measured every 3 days for a timespan of 14 days after initial injection of sEVs. Statistical analysis was performed using ANOVA with post-hoc Tukey's multiple comparisons test, $p < 0.0001$. (c) Tumour weight (g) at time of sacrifice was measured 14 days after initial injection of NgR2-sEVs, Mock-sEVs or PBS. Statistical analysis was performed using ANOVA with post-hoc Tukey's multiple comparisons test, $p < 0.0001$. (d,e) Immunohistochemical (IHC) analysis of DU145 tumours injected with NgR2-sEVs or Mock-sEVs. Tissues were collected at time of sacrifice. Images were captured under 20× magnification; the bars in each image represent 50 μm. (d) Tissues were stained for expression of NgR2; non-immune IgG was used as control. (e) Tissues were stained for expression of Synaptophysin (SYP); non-immune IgG was used as control. (f) EVs were isolated from PC3 NgR2 KO and PC3 Control cells by differential ultracentrifugation and analysed by IB for Abs against NgR2, CD9, TSG101 and CANX. (g) IB analysis of DU145 TCLs collected 24 h after incubation with PC3 NgR2 KO or PC3 Control sEVs; all sEVs were isolated by IDG separation. Samples were analysed for expression of phosphorylated FAK (FAK^{pY397}), tFAK and Actin. (h) Log2 normalized mRNA expression of *RTN4RL2* (NgR2) in PrCa patient-derived serum EVs ($n = 24$) and urine EVs ($n = 7$), tumour tissue ($n = 5$) and normal tissue ($n = 5$). *P*-values were derived via Wilcoxon tests.

(Figure 4b) and weight (Figure 4c) as compared to control Mock-sEVs. Immunohistochemical (IHC) analysis of tumours injected with NgR2-sEVs ($n = 4$) shows increased intensity of NgR2 expression when compared to tumours injected with Mock-sEVs ($n = 3$) (Figure 4d, intensity grading Figure S2, $p = 0.0262$). Synaptophysin (SYP), a marker associated with NEPrCa, is expressed in NgR2-sEV injected tumours ($n = 9$) and is undetectable in Mock-sEV injected tumours ($n = 9$) (Figure 4e). Overall, the result shows that the transfer of NgR2 to recipient cells via sEVs, which is detectable both in vitro (Figure 4a) and in vivo (Figure 4d), increases tumor growth and induces a NE phenotype.

To analyse the impact of sEVs that contain NgR2 on downstream pathway activation, EVs were isolated from PC3 NgR2 CRISPR knock-out (NgR2 KO) cells or PC3 Control cells and analysed by IB with Abs against NgR2, CD9, TSG101 and CANX (Figure 4f). NgR2 expression is downregulated in NgR2 KO EVs when compared to Control EVs. Both NgR2 KO and Control EVs express CD9 and TSG101 and do not express CANX. DU145 cells were then incubated with sEVs, isolated by IDG separation, from NgR2 KO or Control cells. Cells were cultured for 24 h, lysed and analysed by IB for Abs against phosphorylated focal adhesion kinase (FAK^{pY397}), total FAK (tFAK) or Actin (Figure 4g). This result demonstrates that cells incubated with PC3 Control sEVs show increased expression of FAK^{pY397} when compared to NgR2 KO sEVs, while tFAK protein expression levels remain comparable.

Finally, through RNA sequencing analysis of samples characterized by Chen et al. (Chen et al., 2022), we show significant enrichment of *RTN4RL2* (NgR2) in PrCa patient samples (urine-derived EVs, serum-derived EVs and tumour tissue) when compared to normal prostate tissue (Figure 4h). The analysis demonstrates that the *RTN4RL2* mRNA expression reflects the presence of PrCa and could be detected in biofluids via EVs.

3.4 | NgR2 promotes tumour growth

To compare the effect on tumour growth of NgR2-positive sEVs to their cells of origin, we tested the ability of NgR2-expressing cells to promote tumour growth in vivo. We subcutaneously injected SCID mice ($n = 10$) with DU145 cells expressing NgR2 (NgR2-DU145) or Mock (Mock-DU145) transfectants. At day 18, the DU145 PrCa cell transfectants expressing NgR2 form a palpable tumour that continues to grow until euthanasia (day 30) (Figure 5a). At day 30, both tumour volume and weight of NgR2-DU145 tumours are significantly higher than Mock-DU145 tumours (Figure 5a, b). The transfectants analysed by IB show that the levels of the $\alpha V\beta 3$ integrin are comparable in NgR2 and Mock PrCa cells (Figure 5c).

A parallel analysis similarly shows that NgR2 promotes tumour growth; PC3 cells transfected with shRNA against *RTN4RL2* [sh*RTN4RL2*_3 ($n = 6$), sh*RTN4RL2*_2 ($n = 5$) or sh*RTN4RL2*_1 ($n = 5$)], or scramble shRNA ($n = 6$) were injected subcutaneously into SCID mice; the xenografts were collected 17 days after injection. Tumour growth rates were decreased for sh*RTN4RL2* clones when compared to xenografts that express NgR2 (Scramble shRNA) (Figure 5d). The tumour weights, measured at time of sacrifice, show that cells lacking NgR2 expression form tumours at a lower rate than cells expressing NgR2 (Figure 5e). IHC analysis of PC3 tumour tissues collected at 17 days (time of sacrifice) shows reduced expression of NgR2 in sh*RTN4RL2* expressing tumours as compared to scramble shRNA expressing tumours (Figure 5f). These results show that NgR2 promotes tumour growth and its effect is not dependent on altered levels of the $\alpha V\beta 3$ integrin, to which it associates (Quaglia et al., 2022).

4 | DISCUSSION

In this paper, we demonstrate for the first time that the expression of the $\alpha V\beta 3$ integrin in cells results in the formation of LD sEVs, which carry an increased amount of NgR2, a protein known to promote NED. In addition, we provide evidence that NgR2 contributes to tumour growth in vivo and that intratumoral injection of $\alpha V\beta 3$/NgR2+ PrCa sEVs promotes PrCa tumour growth and induces NED. Overall, our findings indicate, as depicted in Figure 6, that sEVs expressing $\alpha V\beta 3$ and NgR2 are key components of PrCa progression.

sEVs contribute to tumour growth by impacting multiple mechanisms, including angiogenesis, cell death evasion and epithelial-mesenchymal transition (Kogure et al., 2020; Möller & Lobb, 2020; Shelton et al., 2018). Their small size allows for both local and systemic distribution throughout the body (Gurung et al., 2021) via both autocrine and paracrine signaling mechanisms (Zhang & Grizzle, 2014). We show that $\alpha V\beta 3$-C4-2B sEVs exhibit increased expression of genes associated with cell proliferation and tumour cell survival compared to Mock-C4-2B sEVs. Our findings indicate that the exogenous expression of $\alpha V\beta 3$ in C4-2B PrCa cells, when compared to Mock control cells, shifts sEVs to a LD subpopulation. It has been reported that LD sEVs and HD sEVs differentially express DNA and proteins (Kowal et al., 2016; Lázaro-Ibáñez et al., 2019). Studies have also shown that LD sEVs and HD sEVs differentially impact recipient cell gene expression (Willms et al., 2016). The relationship between the shift that we observe from a HD to a LD subpopulation and the change in gene expression could potentially play a crucial role in the overall uptake of sEV content by recipient cells.

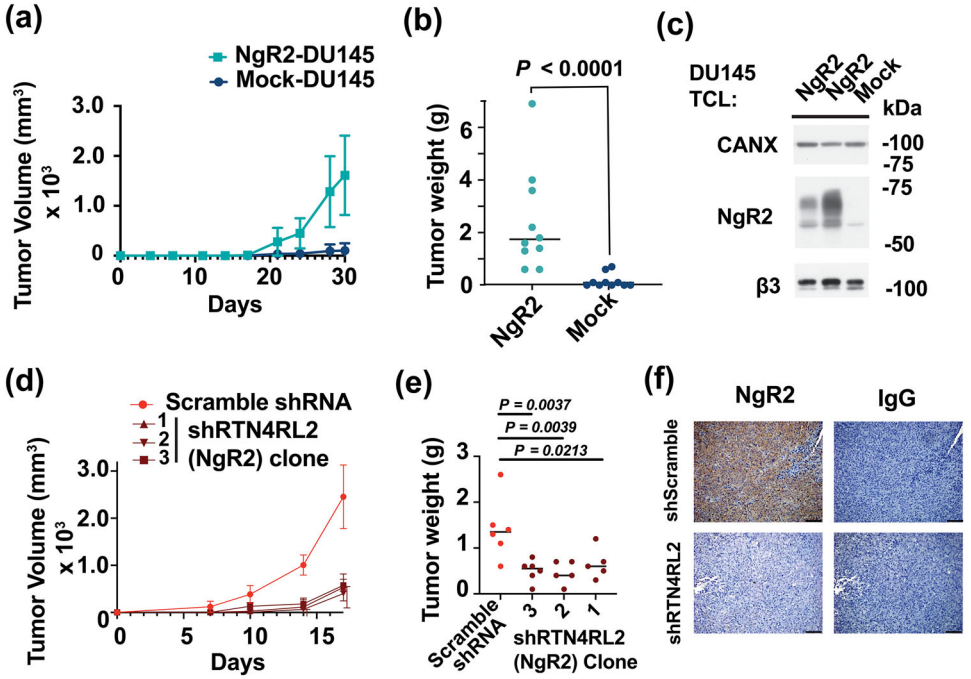

FIGURE 5 NgR2 expression increases tumour growth. (a) Tumour volume measured twice a week for 30 days following subcutaneous injection of Mock-DU145 or NgR2-DU145 cells (2×10^6) in SCID mice ($n = 10$ mice for each group), analysed by mixed effects linear regression, *P*-value for difference in growth rates $p = 0.0002$. (b) Tumour weight 30 days after subcutaneous injection of Mock-DU145 or NgR2-DU145 cells, recorded after sacrifice ($n = 10$ mice for each group), Kruskal Wallis test $p < 0.0001$. (c) IB characterization using Abs to CANX, NgR2 and $\beta3$ for DU145 cells exogenously expressing NgR2. Two populations of NgR2-DU145 cells and one population of Mock-DU145 control cells were analysed. (d) Tumour volume measured twice a week for 17 days following subcutaneous injection of cells expressing NgR2 shRNA compared to control scramble shRNA ($n = 5$–6 mice for each condition). Statistical analysis was performed using ANOVA with post-hoc Dunnett's multiple comparisons test, sh*RTN4RL2*_3 $p = 0.0055$, sh*RTN4RL2*_2 $p = 0.0039$, sh*RTN4RL2*_1 $p = 0.0066$. (e) Tumour weight at time of sacrifice of SCID mice 17 days after subcutaneous injection of PC3 cells expressing NgR2 shRNA compared to control scramble shRNA ($n = 5$–6 mice for each condition). Statistical analysis was performed using ANOVA with post-hoc Dunnett's multiple comparisons test, sh*RTN4RL2*_3 $p = 0.0037$, sh*RTN4RL2*_2 $p = 0.0039$, sh*RTN4RL2*_1 $p = 0.0213$. (f) IHC analysis of shScramble or sh*RTN4RL2* (sh*RTN4RL2*_3) tumour tissues collected at time of sacrifice. Tissues were stained for expression of NgR2; non-immune IgG was used as control. Images were captured under 20x magnification; the bars in each image represent 50 μm.

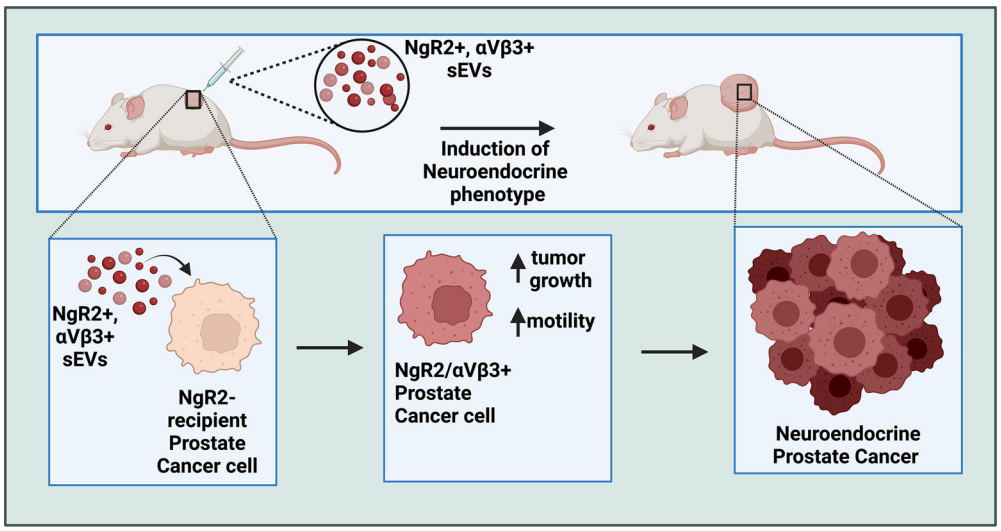

FIGURE 6 Schematic representation of the findings described in this paper. sEVs released from $\alpha V\beta3$+ cancer cells express higher levels of NgR2 as compared to sEVs released from $\alpha V\beta3$- cancer cells. These low-density sEVs show a similar tetraspanin profile whether they express NgR2 or not. sEVs released from $\alpha V\beta3$+ NgR2+ cancer cells are transferred to PrCa recipient cells, which do not express NgR2. Upon sEV transfer, cells that acquire $\alpha V\beta3$ and NgR2 form tumours larger than those without NgR2. Furthermore, the expression of NgR2 and $\alpha V\beta3$ in recipient PrCa cells leads to the induction of a NE phenotype and the development of NEPrCa. Created with BioRender.com.

Specific integrins in sEVs have been identified as novel markers of a multitude of cancers, including prostate, breast and pancreatic cancer (Krishn et al., 2019; Lucotti et al., 2022; Paolillo & Schinelli, 2017). In previous studies, we have reported that the αVβ3 integrin is upregulated in NEPrCa (Quaglia et al., 2020) and that the expression of αVβ3 regulates NgR2 as a driver of NEPrCa progression in vitro (Quaglia et al., 2022). In this manuscript, for the first time, we provide evidence that NgR2 in sEVs drives tumour growth. Although we cannot exclude autocrine mechanisms of sEVs as drivers of tumour growth, paracrine pathways are more relevant due to the cascade of signals from single cells to multiple cells as a major driver of tumour cell differentiation. We investigated the impact of sEVs that express NgR2 in vivo by administering sEVs via intratumoral injection, a method proven effective in sEV studies (Jella et al., 2020; Lu et al., 2022; Peng et al., 2022). In a previous study by Matsumoto et al., a considerable percentage of intratumorally injected radio-labelled melanoma sEVs remained local to tumour tissue and impacted tumour growth (Matsumoto et al., 2017). Another study by Lara et al. showed that the intratumoral injection of fluorescently labelled EVs remained local to the tumour site after 70 h in mice (Lara et al., 2021). In our study, the intratumoral injection of NgR2-positive sEVs allowed for a clear result of their impact on PrCa tumour growth. NgR2 has also been investigated for affecting macrophage efflux after injury and regulating leukocyte infiltration into tissues (Fry et al., 2007; Steinbach et al., 2011). Therefore, we speculate that NgR2-positive sEVs may affect the immune response in PrCa.

The mechanisms underlying the development of NEPrCa, which include the loss of androgen dependence and an increase in neuronal markers, remain unclear (Yamada & Beltran, 2021). Established neuronal markers upregulated in NEPrCa include SYP, chromogranin A and neuron specific enolase; additional neuronal markers associated with NED continue to be identified (Beltran et al., 2011). It is known that the signaling molecule FAK is activated by integrins (Zheng et al., 1999) and its phosphorylation is associated with increased cell survival and inhibition of apoptosis (Cooper et al., 2002). Our results also show that NgR2-sEVs increase FAK activity in recipient cells, while maintaining consistent levels of total FAK expression in vitro. This increased activation of FAK, modulated by NgR2-sEVs, may contribute to tumour progression.

The effect of αVβ3 is well-known in cancer progression and includes angiogenesis, migration and association with growth factor receptors (Ludwig et al., 2021). It is also known that tumour cells expressing αVβ3 in specific activation states contribute to tumour cell extravasation and metastasis (Weber et al., 2016). Treatments that specifically target the αVβ3 integrin have also been reported to be effective at inhibiting PrCa progression (Jiang et al., 2017). In contrast, the role of NgR2 in cancer progression has been minimally reported (Osman et al., 2021; Quaglia et al., 2022). In this study, we conclude that αVβ3 expression is crucial for NgR2 expression in sEVs. Previous reports have established NgR2 as having multiple purposes in neuronal functions, including the regulation of axonal growth and dendritic cell adhesion to myelin (Barton et al., 2003; McDonald et al., 2011). Our report shows that αVβ3 is required for NgR2 expression in both cells and sEVs and suggests that their interactions in sEVs may control their impact on recipient cell uptake in the tumour microenvironment. There is debate on whether αVβ3 is required for sEV uptake; previous studies have shown that αVβ3 expression in cells is a crucial component to sEV uptake and relies on the interactions with proteins such as dynamin and FAK (Altei et al., 2020; Fuentes et al., 2020); in contrast, our laboratory has reported that αVβ3 expression in sEVs is not required for recipient cell uptake (Krishn et al., 2019). Whether the interaction of the αVβ3 integrin with NgR2 in cells is essential for sEV uptake in recipient cells requires further investigation.

AUTHOR CONTRIBUTIONS

Cecilia E. Verrillo: Formal analysis; investigation; methodology; writing—original draft; writing—review and editing. **Fabio Quaglia**: Formal analysis; investigation; methodology; writing—original draft; writing—review and editing. **Christopher D. Shields**: Formal analysis; investigation; methodology; writing—review and editing. **Stephen Lin**: Formal analysis; investigation; methodology; writing—review and editing. **Andrew V. Kossenkov**: Data curation; formal analysis; writing—original draft; writing—review and editing. **Hsin-Yao Tang**: Formal analysis; investigation; methodology; writing—original draft. **David Speicher**: Investigation; methodology. **Nicole M. Naranjo**: Formal analysis; writing—review and editing. **Anna Testa**: Formal analysis; writing—review and editing. **William K. Kelly**: Formal analysis; writing—review and editing. **Qin Liu**: Data curation; validation; writing—original draft; writing—review and editing. **Benjamin Leiby**: Data curation; validation; writing—original draft; writing—review and editing. **Luca Musante**: Data curation; formal analysis. **Khalid Sossey-Alaoui**: Formal analysis; writing—review and editing. **Navneet Dogra**: Formal analysis; investigation; methodology; writing—review and editing. **Tzu-Yi Chen**: Formal analysis; investigation; methodology; writing—review and editing. **Dario C. Altieri**: Formal analysis; writing—review and editing. **Lucia R. Languino**: Formal analysis; funding acquisition; investigation; methodology; project administration; supervision; writing—original draft; writing—review and editing.

ACKNOWLEDGEMENTS

The authors would like to thank Dr. George Daaboul at Nanoview Biosciences for protocol guidance. We would also like to thank Dr. Wei Jiang and Dr. Zhijiu Zhong of the Sidney Kimmel Cancer Center (SKCC) Translational Research/Pathology Facility at Thomas Jefferson University for technical support with immunohistochemistry experiments; Dr. Larry Harshyne III and Thomas Cantrell of the SKCC Flow Cytometry and Human Immune Monitoring Core at Thomas Jefferson University for technical support with NTA. This study was supported by R01 CA224769 and DoD W81XWH2210826 (to LRL), and Prostate Cancer Foundation Young Investigator Award 2021 (to FQ and AT), Philadelphia Prostate Cancer Biome Project (to LRL), R01CA217329

and R01CA255792 (to WKK). AT is a Visiting Scholar at Thomas Jefferson University, partially funded by the University of Turin, Italy. The research reported in this publication utilized the Flow Cytometry and Human Immune Monitoring Core and the Translational Research/Pathology Shared Resource, and the Biostatistics, Bioinformatics and Research Informatics Shared Resource at the Sidney Kimmel Cancer Center (Thomas Jefferson University, Philadelphia, PA) that the NCI supports under award number P30CA056036. KSA was supported by a startup fund from MetroHealth System. AVK was supported by NCI R50 CA211199. HYT was supported by NCI R50 CA221838. Support for the Wistar Proteomics and Metabolomics Core Facility was provided by Cancer Center Support Grant CA010815. ND was supported by P20CA264076; ND and TYC were supported by R21 AG078848. DCA was supported by R35CA220446.

CONFLICT OF INTEREST STATEMENT

F.Q. is an employee of Janssen. No potential conflict of interest was reported by the other author(s).

ORCID

Navneet Dogra https://orcid.org/0000-0002-4602-3991
Lucia R. Languino https://orcid.org/0000-0001-9011-7031

REFERENCES

Altei, W. F., Pachane, B. C., Santos, P. K. D., Ribeiro, L. N. M., Sung, B. H., Weaver, A. M., & Selistre-de-Araújo, H. S. (2020). Inhibition of αvβ3 integrin impairs adhesion and uptake of tumor-derived small extracellular vesicles. *Cell Communication and Signaling: CCS*, *18*(1), 158.

Barton, W. A., Liu, B. P., Tzvetkova, D., Jeffrey, P. D., Fournier, A. E., Sah, D., Cate, R., Strittmatter, S. M., & Nikolov, D. B. (2003). Structure and axon outgrowth inhibitor binding of the Nogo-66 receptor and related proteins. *The EMBO Journal*, *22*(13), 3291–3302.

Bäumer, B. E., Kurz, A., Borrie, S. C., Sickinger, S., Dours-Zimmermann, M. T., Zimmermann, D. R., & Bandtlow, C. E. (2014). Nogo receptor homolog NgR2 expressed in sensory DRG neurons controls epidermal innervation by interaction with Versican. *The Journal of Neuroscience: The Official Journal of the Society for Neuroscience*, *34*(5), 1633–1646.

Beltran, H., Prandi, D., Mosquera, J. M., Benelli, M., Puca, L., Cyrta, J., Marotz, C., Giannopoulou, E., Chakravarthi, B. V., Varambally, S., Tomlins, S. A., Nanus, D. M., Tagawa, S. T., Van Allen, E. M., Elemento, O., Sboner, A., Garraway, L. A., Rubin, M. A., & Demichelis, F. (2016). Divergent clonal evolution of castration-resistant neuroendocrine prostate cancer. *Nature Medicine*, *22*(3), 298–305.

Beltran, H., Rickman, D. S., Park, K., Chae, S. S., Sboner, A., MacDonald, T. Y., Wang, Y., Sheikh, K. L., Terry, S., Tagawa, S. T., Dhir, R., Nelson, J. B., de la Taille, A., Allory, Y., Gerstein, M. B., Perner, S., Pienta, K. J., Chinnaiyan, A. M., Wang, Y., … & Rubin, M. A. (2011). Molecular characterization of neuroendocrine prostate cancer and identification of new drug targets. *Cancer Discovery*, *1*(6), 487–495.

Blavier, L., Nakata, R., Neviani, P., Sharma, K., Shimada, H., Benedicto, A., Matei, I., Lyden, D., & DeClerck, Y. A. (2023). The capture of extracellular vesicles endogenously released by xenotransplanted tumours induces an inflammatory reaction in the premetastatic niche. *Journal of Extracellular Vesicles*, *12*(5), e12326.

Bledzka, K., Bialkowska, K., Sossey-Alaoui, K., Vaynberg, J., Pluskota, E., Qin, J., & Plow, E. F. (2016). Kindlin-2 directly binds actin and regulates integrin outside-in signaling. *The Journal of cell biology*, *213*(1), 97–108.

Carlson, P., Dasgupta, A., Grzelak, C. A., Kim, J., Barrett, A., Coleman, I. M., Shor, R. E., Goddard, E. T., Dai, J., Schweitzer, E. M., Lim, A. R., Crist, S. B., Cheresh, D. A., Nelson, P. S., Hansen, K. C., & Ghajar, C. M. (2019). Targeting the perivascular niche sensitizes disseminated tumour cells to chemotherapy. *Nature Cell Biology*, *21*(2), 238–250.

Chen, T. Y., Gonzalez-Kozlova, E., Soleymani, T., La Salvia, S., Kyprianou, N., Sahoo, S., Tewari, A. K., Cordon-Cardo, C., Stolovitzky, G., & Dogra, N. (2022). Extracellular vesicles carry distinct proteo-transcriptomic signatures that are different from their cancer cell of origin. *Iscience*, *25*(6), 104414.

Cooper, C. R., Chay, C. H., & Pienta, K. J. (2002). The role of alpha(v)beta(3) in prostate cancer progression. *Neoplasia (New York, N.Y.)*, *4*(3), 191–194.

Cox, J., & Mann, M. (2008). MaxQuant enables high peptide identification rates, individualized p.p.b.-range mass accuracies and proteome-wide protein quantification. *Nature Biotechnology*, *26*(12), 1367–1372.

Deng, F., Ratri, A., Deighan, C., Daaboul, G., Geiger, P. C., & Christenson, L. K. (2022). Single-particle interferometric reflectance imaging characterization of individual extracellular vesicles and population dynamics. *Journal of Visualized Experiments: JoVE*, (179), e62988.

Desgrosellier, J. S., & Cheresh, D. A. (2010). Integrins in cancer: Biological implications and therapeutic opportunities. *Nature Reviews. Cancer*, *10*(1), 9–22.

Fry, E. J., Ho, C., & David, S. (2007). A role for Nogo receptor in macrophage clearance from injured peripheral nerve. *Neuron*, *53*(5), 649–662.

Fuentes, P., Sesé, M., Guijarro, P. J., Emperador, M., Sánchez-Redondo, S., Peinado, H., Hümmer, S., & Ramón Y Cajal, S. (2020). ITGB3-mediated uptake of small extracellular vesicles facilitates intercellular communication in breast cancer cells. *Nature Communications*, *11*(1), 4261.

García-Silva, S., Benito-Martín, A., Nogués, L., Hernández-Barranco, A., Mazariegos, M. S., Santos, V., Hergueta-Redondo, M., Ximénez-Embún, P., Kataru, R. P., Lopez, A. A., Merino, C., Sánchez-Redondo, S., Graña-Castro, O., Matei, I., Nicolás-Avila, J. Á., Torres-Ruiz, R., Rodríguez-Perales, S., Martínez, L., Pérez-Martínez, M., … & Peinado, H. (2021). Melanoma-derived small extracellular vesicles induce lymphangiogenesis and metastasis through an NGFR-dependent mechanism. *Nature Cancer*, *2*(12), 1387–1405.

Gurung, S., Perocheau, D., Touramanidou, L., & Baruteau, J. (2021). The exosome journey: From biogenesis to uptake and intracellular signaling. *Cell Communication and Signaling: CCS*, *19*(1), 47.

Hao, X., Zhao, B., Towers, M., Liao, L., Monteiro, E. L., Xu, X., Freeman, C., Peng, H., Tang, H. Y., Havas, A., Kossenkov, A. V., Berger, S. L., Adams, P. D., Speicher, D. W., Schultz, D., Marmorstein, R., Zaret, K. S., & Zhang, R. (2024). TXNRD1 drives the innate immune response in senescent cells with implications for age-associated inflammation. *Nature Aging*, *4*(2), 185–197.

Hoshino, A., Costa-Silva, B., Shen, T. L., Rodrigues, G., Hashimoto, A., Tesic Mark, M., Molina, H., Kohsaka, S., Di Giannatale, A., Ceder, S., Singh, S., Williams, C., Soplop, N., Uryu, K., Pharmer, L., King, T., Bojmar, L., Davies, A. E., Ararso, Y., … & Lyden, D. (2015). Tumour exosome integrins determine organotropic metastasis. *Nature*, *527*(7578), 329–335.

Jella, K. K., Nasti, T. H., Li, Z., Lawson, D. H., Switchenko, J. M., Ahmed, R., Dynan, W. S., & Khan, M. K. (2020). Exosome-containing preparations from postirradiated mouse melanoma cells delay melanoma growth in vivo by a natural killer cell-dependent mechanism. *International Journal of Radiation Oncology, Biology, Physics*, *108*(1), 104–114.

Jiang, Y., Dai, J., Yao, Z., Shelley, G., & Keller, E. T. (2017). Abituzumab targeting of αV-class integrins inhibits prostate cancer progression. *Molecular Cancer Research: MCR*, *15*(7), 875–883.

Kogure, A., Yoshioka, Y., & Ochiya, T. (2020). Extracellular vesicles in cancer metastasis: Potential as therapeutic targets and materials. *International Journal of Molecular Sciences*, *21*(12), 4463.

Kowal, J., Arras, G., Colombo, M., Jouve, M., Morath, J. P., Primdal-Bengtson, B., Dingli, F., Loew, D., Tkach, M., & Théry, C. (2016). Proteomic comparison defines novel markers to characterize heterogeneous populations of extracellular vesicle subtypes. *Proceedings of the National Academy of Sciences of the United States of America*, *113*(8), E968–E977.

Krämer, A., Green, J., Pollard, J., Jr, & Tugendreich, S. (2014). Causal analysis approaches in ingenuity pathway analysis. *Bioinformatics (Oxford, England)*, *30*(4), 523–530.

Krishn, S. R., Salem, I., Quaglia, F., Naranjo, N. M., Agarwal, E., Liu, Q., Sarker, S., Kopenhaver, J., McCue, P. A., Weinreb, P. H., Violette, S. M., Altieri, D. C., & Languino, L. R. (2020). The αvβ6 integrin in cancer cell-derived small extracellular vesicles enhances angiogenesis. *Journal of Extracellular Vesicles*, *9*(1), 1763594.

Krishn, S. R., Singh, A., Bowler, N., Duffy, A. N., Friedman, A., Fedele, C., Kurtoglu, S., Tripathi, S. K., Wang, K., Hawkins, A., Sayeed, A., Goswami, C. P., Thakur, M. L., Iozzo, R. V., Peiper, S. C., Kelly, W. K., & Languino, L. R. (2019). Prostate cancer sheds the αvβ3 integrin in vivo through exosomes. *Matrix Biology: Journal of the International Society for Matrix Biology*, *77*, 41–57.

Lara, P., Huis In 't Veld, R. V., Jorquera-Cordero, C., Chan, A. B., Ossendorp, F., & Cruz, L. J. (2021). Zinc-phthalocyanine-loaded extracellular vesicles increase efficacy and selectivity of photodynamic therapy in co-culture and preclinical models of colon cancer. *Pharmaceutics*, *13*(10), 1547.

Lázaro-Ibáñez, E., Lässer, C., Shelke, G. V., Crescitelli, R., Jang, S. C., Cvjetkovic, A., García-Rodríguez, A., & Lötvall, J. (2019). DNA analysis of low- and high-density fractions defines heterogeneous subpopulations of small extracellular vesicles based on their DNA cargo and topology. *Journal of Extracellular Vesicles*, *8*(1), 1656993.

Lu, H., Wang, T., Li, J., Fedele, C., Liu, Q., Zhang, J., Jiang, Z., Jain, D., Iozzo, R. V., Violette, S. M., Weinreb, P. H., Davis, R. J., Gioeli, D., FitzGerald, T. J., Altieri, D. C., & Languino, L. R. (2016). αvβ6 integrin promotes castrate-resistant prostate cancer through JNK1-mediated activation of androgen receptor. *Cancer Research*, *76*(17), 5163–5174.

Lu, Y., Cao, G., Lan, H., Liao, H., Hu, Y., Feng, H., Liu, X., & Huang, P. (2022). Chondrocyte-derived exosomal miR-195 inhibits osteosarcoma cell proliferation and anti-apoptotic by targeting KIF4A in vitro and in vivo. *Translational Oncology*, *16*, 101289.

Lucotti, S., Kenific, C. M., Zhang, H., & Lyden, D. (2022). Extracellular vesicles and particles impact the systemic landscape of cancer. *The EMBO Journal*, *41*(18), e109288.

Ludwig, B. S., Kessler, H., Kossatz, S., & Reuning, U. (2021). RGD-binding integrins revisited: how recently discovered functions and novel synthetic ligands (re-)shape an ever-evolving field. *Cancers*, *13*(7), 1711.

Mathieu, M., Martin-Jaular, L., Lavieu, G., & Théry, C. (2019). Specificities of secretion and uptake of exosomes and other extracellular vesicles for cell-to-cell communication. *Nature Cell Biology*, *21*(1), 9–17.

Matsumoto, A., Takahashi, Y., Nishikawa, M., Sano, K., Morishita, M., Charoenviriyakul, C., Saji, H., & Takakura, Y. (2017). Accelerated growth of B16BL6 tumor in mice through efficient uptake of their own exosomes by B16BL6 cells. *Cancer Science*, *108*(9), 1803–1810.

McDonald, C. L., Steinbach, K., Kern, F., Schweigreiter, R., Martin, R., Bandtlow, C. E., & Reindl, M. (2011). Nogo receptor is involved in the adhesion of dendritic cells to myelin. *Journal of neuroinflammation*, *8*, 113.

Möller, A., & Lobb, R. J. (2020). The evolving translational potential of small extracellular vesicles in cancer. *Nature reviews. Cancer*, *20*(12), 697–709.

Nam, A., Jain, S., Wu, C., Campos, A., Shepard, R. M., Yu, Z., Reddy, J. P., Von Schalscha, T., Weis, S. M., Onaitis, M., Wettersten, H. I., & Cheresh, D. A. (2024). Integrin αvβ3 upregulation in response to nutrient stress promotes lung cancer cell metabolic plasticity. *Cancer Research*, *84*(10), 1630–1642.

Noren Hooten, N., Yáñez-Mó, M., DeRita, R., Russell, A., Quesenberry, P., Ramratnam, B., Robbins, P. D., Di Vizio, D., Wen, S., Witwer, K. W., & Languino, L. R. (2020). Hitting the bullseye: Are extracellular vesicles on target? *Journal of Extracellular Vesicles*, *10*(1), e12032.

Osman, Y., Elsharkawy, T., Hashim, T. M., Alratroot, J. A., Alsuwat, H. S., Otaibi, W. M. A., Hegazi, F. M., AbdulAzeez, S., & Borgio, J. F. (2021). Functional multigenic variations associated with hodgkin lymphoma. *International Journal of Laboratory Hematology*, *43*(6), 1472–1482.

Paolillo, M., & Schinelli, S. (2017). Integrins and exosomes, a dangerous liaison in cancer progression. *Cancers*, *9*(8), 95.

Peinado, H., Zhang, H., Matei, I. R., Costa-Silva, B., Hoshino, A., Rodrigues, G., Psaila, B., Kaplan, R. N., Bromberg, J. F., Kang, Y., Bissell, M. J., Cox, T. R., Giaccia, A. J., Erler, J. T., Hiratsuka, S., Ghajar, C. M., & Lyden, D. (2017). Pre-metastatic niches: Organ-specific homes for metastases. *Nature Reviews. Cancer*, *17*(5), 302–317.

Peng, B., Nguyen, T. M., Jayasinghe, M. K., Gao, C., Pham, T. T., Vu, L. T., Yeo, E. Y. M., Yap, G., Wang, L., Goh, B. C., Tam, W. L., Luo, D., & Le, M. T. (2022). Robust delivery of RIG-I agonists using extracellular vesicles for anti-cancer immunotherapy. *Journal of Extracellular Vesicles*, *11*(4), e12187.

Quaglia, F., Krishn, S. R., Daaboul, G. G., Sarker, S., Pippa, R., Domingo-Domenech, J., Kumar, G., Fortina, P., McCue, P., Kelly, W. K., Beltran, H., Liu, Q., & Languino, L. R. (2020). Small extracellular vesicles modulated by αVβ3 integrin induce neuroendocrine differentiation in recipient cancer cells. *Journal of Extracellular Vesicles*, *9*(1), 1761072.

Quaglia, F., Krishn, S. R., Sossey-Alaoui, K., Rana, P. S., Pluskota, E., Park, P. H., Shields, C. D., Lin, S., McCue, P., Kossenkov, A. V., Wang, Y., Goodrich, D. W., Ku, S. Y., Beltran, H., Kelly, W. K., Corey, E., Klose, M., Bandtlow, C., Liu, Q., … & Languino, L. R. (2022). The NOGO receptor NgR2, a novel αVβ3 integrin effector, induces neuroendocrine differentiation in prostate cancer. *Scientific Reports*, *12*(1), 18879.

Quaglia, F., Krishn, S. R., Wang, Y., Goodrich, D. W., McCue, P., Kossenkov, A. V., Mandigo, A. C., Knudsen, K. E., Weinreb, P. H., Corey, E., Kelly, W. K., & Languino, L. R. (2021). Differential expression of αVβ3 and αVβ6 integrins in prostate cancer progression. *PLoS ONE*, *16*(1), e0244985.

Ritchie, M. E., Phipson, B., Wu, D., Hu, Y., Law, C. W., Shi, W., & Smyth, G. K. (2015). limma powers differential expression analyses for RNA-sequencing and microarray studies. *Nucleic Acids Research*, *43*(7), e47.

Schmidt, L. J., Duncan, K., Yadav, N., Regan, K. M., Verone, A. R., Lohse, C. M., Pop, E. A., Attwood, K., Wilding, G., Mohler, J. L., Sebo, T. J., Tindall, D. J., & Heemers, H. V. (2012). RhoA as a mediator of clinically relevant androgen action in prostate cancer cells. *Molecular Endocrinology (Baltimore, Md.)*, *26*(5), 716–735.

Shelton, P. M., Duran, A., Nakanishi, Y., Reina-Campos, M., Kasashima, H., Llado, V., Ma, L., Campos, A., García-Olmo, D., García-Arranz, M., García-Olmo, D. C., Olmedillas-López, S., Caceres, J. F., Diaz-Meco, M. T., & Moscat, J. (2018). The secretion of miR-200s by a PKCζ/ADAR2 signaling axis promotes liver metastasis in colorectal cancer. *Cell Reports*, *23*(4), 1178–1191.

Siegel, R. L., Giaquinto, A. N., & Jemal, A. (2024). Cancer statistics, 2024. *CA: A Cancer Journal for Clinicians*, *74*(1), 12–49.

Singh, A., Fedele, C., Lu, H., Nevalainen, M. T., Keen, J. H., & Languino, L. R. (2016). Exosome-mediated transfer of αvβ3 integrin from tumorigenic to nontumorigenic cells promotes a migratory phenotype. *Molecular Cancer Research: MCR*, *14*(11), 1136–1146.

Steinbach, K., McDonald, C. L., Reindl, M., Schweigreiter, R., Bandtlow, C., & Martin, R. (2011). Nogo-receptors NgR1 and NgR2 do not mediate regulation of CD4 T helper responses and CNS repair in experimental autoimmune encephalomyelitis. *PLoS ONE*, *6*(11), e26341.

Testa, A., Quaglia, F., Naranjo, N. M., Verrillo, C. E., Shields, C. D., Lin, S., Pickles, M. W., Hamza, D. F., Von Schalscha, T., Cheresh, D. A., Leiby, B., Liu, Q., Ding, J., Kelly, W. K., Hooper, D. C., Corey, E., Plow, E. F., Altieri, D. C., & Languino, L. R. (2023). Targeting the $\alpha V\beta 3$/NgR2 pathway in neuroendocrine prostate cancer. *Matrix Biology: Journal of the International Society For Matrix Biology*, *124*, 49–62.

Trerotola, M., Jernigan, D. L., Liu, Q., Siddiqui, J., Fatatis, A., & Languino, L. R. (2013). Trop-2 promotes prostate cancer metastasis by modulating $\beta(1)$ integrin functions. *Cancer Research*, *73*(10), 3155–3167.

Urabe, F., Kosaka, N., Kimura, T., Egawa, S., & Ochiya, T. (2018). Extracellular vesicles: Toward a clinical application in urological cancer treatment. *International Journal of Urology: Official Journal of The Japanese Urological Association*, *25*(6), 533–543.

Urabe, F., Yamada, Y., Yamamoto, S., Tsuzuki, S., Kimura, S., Ochiya, T., & Kimura, T. (2024). Extracellular vesicles and prostate cancer management: A narrative review. *Translational Andrology and Urology*, *13*(3), 442–453.

Venkatesh, K., Chivatakarn, O., Lee, H., Joshi, P. S., Kantor, D. B., Newman, B. A., Mage, R., Rader, C., & Giger, R. J. (2005). The Nogo-66 receptor homolog NgR2 is a sialic acid-dependent receptor selective for myelin-associated glycoprotein. *The Journal of Neuroscience: The Official Journal of the Society for Neuroscience*, *25*(4), 808–822.

Weber, M. R., Zuka, M., Lorger, M., Tschan, M., Torbett, B. E., Zijlstra, A., Quigley, J. P., Staflin, K., Eliceiri, B. P., Krueger, J. S., Marchese, P., Ruggeri, Z. M., & Felding, B. H. (2016). Activated tumor cell integrin $\alpha v\beta 3$ cooperates with platelets to promote extravasation and metastasis from the blood stream. *Thrombosis Research*, *140*, (Suppl 1), S27–S36.

Welsh, J. A., Goberdhan, D. C. I., O'Driscoll, L., Buzas, E. I., Blenkiron, C., Bussolati, B., Cai, H., Di Vizio, D., Driedonks, T. A. P., Erdbrügger, U., Falcon-Perez, J. M., Fu, Q. L., Hill, A. F., Lenassi, M., Lim, S. K., Mahoney, M. G., Mohanty, S., Möller, A., Nieuwland, R., … & Witwer, K. W. (2024). Minimal information for studies of extracellular vesicles (MISEV2023): From basic to advanced approaches. *Journal of Extracellular Vesicles*, *13*(2), e12404.

Willms, E., Johansson, H. J., Mäger, I., Lee, Y., Blomberg, K. E., Sadik, M., Alaarg, A., Smith, C. I., Lehtiö, J., El Andaloussi, S., Wood, M. J., & Vader, P. (2016). Cells release subpopulations of exosomes with distinct molecular and biological properties. *Scientific Reports*, *6*, 22519.

Yamada, Y., & Beltran, H. (2021). Clinical and biological features of neuroendocrine prostate cancer. *Current Oncology Reports*, *23*(2), 15.

Zhang, H. G., & Grizzle, W. E. (2014). Exosomes: A novel pathway of local and distant intercellular communication that facilitates the growth and metastasis of neoplastic lesions. *The American Journal of Pathology*, *184*(1), 28–41.

Zheng, D. Q., Woodard, A. S., Fornaro, M., Tallini, G., & Languino, L. R. (1999). Prostatic carcinoma cell migration via alpha(v)beta3 integrin is modulated by a focal adhesion kinase pathway. *Cancer Research*, *59*(7), 1655–1664.

SUPPORTING INFORMATION

Additional supporting information can be found online in the Supporting Information section at the end of this article.

How to cite this article: Verrillo, C. E., Quaglia, F., Shields, C. D., Lin, S., Kossenkov, A. V., Tang, H.-Y., Speicher, D., Naranjo, N. M., Testa, A., Kelly, W. K., Liu, Q., Leiby, B., Musante, L., Sossey-Alaoui, K., Dogra, N., Chen, T.-Y., Altieri, D. C., & Languino, L. R. (2024). Expression of the $\alpha V\beta 3$ integrin affects prostate cancer sEV cargo and density and promotes sEV pro-tumorigenic activity *in vivo* through a GPI-anchored receptor, NgR2. *Journal of Extracellular Vesicles*, *13*, e12482. https://doi.org/10.1002/jev2.12482